JOINT ANGLE AND DELAY ESTIMATION FOR DS-CDMA WITH APPLICATION TO REDUCED DIMENSION SPACE-TIME RAKE RECEIVERS †

Yung-Fang Chen and Michael D. Zoltowski

School of Electrical and Computer Engineering
Purdue University
West Lafayette, IN 47907-1285
e-mail: yungfang@ecn.purdue.edu, mikedz@ecn.purdue.edu

ABSTRACT

In this paper, we propose an algorithm for joint estimation of the angle of arrival (AOA) and delay of each dominant multipath for the desired user for use in a reduced dimension space-time RAKE receiver for DS-CDMA communications that is "near-far" resistant. After we estimate the desired spatio-frequency signal vector, we propose the 2D unitary ESPRIT algorithm as our estimator which provides closed-form as well as automatically paired AOA-delay estimates. We effectively have a single snapshot of 2D data and thus require 2D smoothing for extracting multiple snapshots. The comparative performance of two 2D smoothing schemes, pre-eigenanalysis and post-eigenanalysis 2D smoothing, is discussed. The space-time data model for the IS-95 uplink is presented. The performance of a reduced dimension space-time RAKE receiver for the IS-95 uplink using the AOA-delay estimates is assessed through Monte-Carlo simulations.

1. INTRODUCTION

In this paper, we present joint angle and delay estimation algorithms for both classical DS-CDMA communication systems and the IS-95 uplink, assuming known spreading waveform of the desired user and approximate bit synchronization. Our algorithm can accurately estimate the angle of arrival (AOA) and time delay for each multipath component of the desired user even under "near-far" conditions. We propose the 2D Unitary ESPRIT algorithm [1] as our estimator which provides closed-form and automatically paired 2D parameter estimates. A major benefit of the joint estimation algorithm is that the number of multipaths can be larger than the number of antennas, which overcomes the limitation of separable estimation. We also present the utility of the joint angle-delay estimates in a reduced dimension space-time RAKE receiver. The AOA information is also useful for FDD downlink beamforming or geolocation.

2. SPACE-TIME DATA MODEL FOR IS-95 UPLINK

We omit the detailed discussion of the IS-95 uplink transmitter structure due to limited space. We adopt the space-time data model for IS-95 uplink discribed in [2]. The j-th symbol transmitted by the i-th user is described as

$$\begin{aligned} \mathrm{s}_i(t) &= \sqrt{P_i}W_i^j(t)a_i^{\mathbf{I}}(t)cos(\omega_c t) + \\ &\quad \sqrt{P_i}W_i^j(t-\frac{T_c}{2})a_i^{\mathbf{Q}}(t-\frac{T_c}{2})sin(\omega_c t) \\ &\quad 0 \le t \le T_w \end{aligned} \qquad (1)$$

The various quantities in (1) are described below. Define $W_i^j(t)$ as Walsh symbol, and j is referred to as the Walsh function index: $j = 1, 2, .., 64$. P_i is the transmitted power per symbol. ω_c is the carrier frequency in radians. T_w is the duration of a Walsh symbol. $a_i^I(t)$ and $a_i^Q(t)$ are the PN spreading codes applied to the I and Q channels, respectively:

$$a_i^I(t) = c_i(t)a^I(t) \qquad a_i^Q(t) = c_i(t)a^Q(t)$$

where $c_i(t)$ is the i-th user spreading waveform and $a^I(t)$,$a^Q(t)$ are two short codes. Denoting the chip waveform as $p(t)$,

$$a_i^I(t) = \sum_{n=-\infty}^{\infty} a_{i,n}^I p(t-nT_c) \ ; \ a_i^Q(t) = \sum_{n=-\infty}^{\infty} a_{i,n}^Q p(t-nT_c), \qquad (2)$$

where $a_{i,n}^I$ and $a_{i,n}^Q$ are distinct PN sequences.

The baseband representation of the $M \times 1$ array snapshot vector $\mathbf{x}(t)$ containing the outputs of each of the M antennas comprising the array at time t is modeled as

$$\begin{aligned} \mathbf{x}(t) = &\sum_{k=1}^{K_d} \rho_k^d \mathbf{a}(\theta_k^d)[W_d^j(t-\tau_k^d)a_d^{\mathbf{I}}(t-\tau_k^d) + \\ &jW_d^j(t-\frac{T_c}{2}-\tau_k^d)a_d^{\mathbf{Q}}(t-\frac{T_c}{2}-\tau_k^d)] + \\ &\sum_{i=1}^{J}\sum_{k=1}^{K_i} \rho_k^i \mathbf{a}(\theta_k^i)[W_i^j(t-\tau_k^i)a_i^{\mathbf{I}}(t-\tau_k^i) + \\ &jW_i^j(t-\frac{T_c}{2}-\tau_k^i)a_i^{\mathbf{Q}}(t-\frac{T_c}{2}-\tau_k^i)] + \mathbf{n}_w(t) \end{aligned} \qquad (3)$$

where d denotes the desired user. $\mathbf{a}(\theta)$ is the spatial response of the array. For the sake of notational simplicity, we assume here that the spatial response vector depends on a single directional parameter, θ, the AOA of a given source. For a given user i: K_i is the number of different paths the i-th signal arrives from, θ_k^i denotes the arrival direction of the k-th multipath, and τ_k^i is the corresponding relative delay of the k-th multipath. ρ_k^i is the complex amplitude of the k-th multipath arrival for the i-th signal at the reference element. J multi-user access interferers (MUAI) impinge upon the array. The vector $\mathbf{n}_w(t)$ represents the contribution of additive white noise. The data model is easily modified for classical DS-CDMA communication systems. The attendant discussion is therefore omitted.

† This research work was supported by AFOSR under contract no. F49620-97-1-0275, the National Science Foundation under grant no. MIPS-9708309, and by Army Research Office Focused Research Initiative under grant no. DAAH04-95-1-0246.

3. JOINT ANGLE AND DELAY ESTIMATION

Our goal is to jointly estimate the AOA and relative delay parameter pairs $\{(\theta_i^d, \tau_i^d)\}, i = 1, \cdots, K_d$, under multipath propagation and "near-far" conditions. We consider applying the 2D Unitary ESPRIT algorithm to the data model formulated in such a way as to exhibit the shift-invariance property required by ESPRIT. The desired data model may be achieved by adapting the space-frequency 2D processing scheme previously proposed by Zoltowski[3]. This 2D RAKE receiver was proposed for direct sequence spread spectrum communication systems and achieve two primary goals: (1) optimal combination of the desired user's multipath in a RAKE-like receiver fashion and (2) simultaneous cancellation of strong multi-user access interference and other forms of interference. It only exploits: (1) known spreading waveform of desired user, (2) approximate bit synchronization for desired user and (3) known maximum multipath time-delay spread τ_{max}. For the 64-ary orthogonal modulation used in the IS-95 uplink, we need to contruct 64 matched filters forming a filter bank at each antenna receiver. Therefore, this matrix pencil is estimated from the aforementioned matched filter outputs containing the "fingers" in a decision directed fashion [3,4].

As shown in [3], after passing the output of each antenna through a matched filter, whose impulse response is an oversampled version of the time-reverse and conjugate of the spreading waveform of the desired user, one estimates the signal plus interference space-frequency correlation matrix, $\hat{\mathbf{K}}_{S+I}$, during that portion of the bit interval where the RAKE fingers occur, and the interference alone space-frequency correlation matrix, $\hat{\mathbf{K}}_I$, during that portion of the bit interval away from the fingers. The optimum weight vector $\hat{\mathbf{w}}_{opt}$ for combining the L spectrum values computed from the N_s pt. DFT of a time window with N_s time samples encompassing the "fingers" at each of the M antennas is the "largest" generalized eigenvector of the $ML \times ML$ space-frequency matrix pencil $\{\hat{\mathbf{K}}_{S+I}, \hat{\mathbf{K}}_I\}$, which is the solution to the SINR maximizing criterion:

$$\underset{\mathbf{w}}{\text{Maximize}} \quad \frac{\mathbf{w}^H \mathbf{K}_{S+I} \mathbf{w}}{\mathbf{w}^H \mathbf{K}_I \mathbf{w}}$$

The asymptotic structure of $\hat{\mathbf{K}}_{S+I}$ may be expressed as:

$$\mathbf{K}_{S+I} = \sigma_s \Big(\sum_{i=1}^{K_d} g_i \mathbf{f}(\tau_i) \otimes \mathbf{a}(\theta_i)\Big)\Big(\sum_{i=1}^{K_d} g_i \mathbf{f}(\tau_i) \otimes \mathbf{a}(\theta_i)\Big)^H + \mathbf{K}_I \tag{4}$$

where we have dropped superscript d for notational simplicity. Assuming the antenna elements to be equi-spaced along a line and well-calibrated, g_i is the complex gain of the i-th multipath arrival, τ_i is the relative time-delay of the i-th multipath arrival, and $\mathbf{a}(\theta_i)$ is the array manifold $= [1, e^{j\mu}, \cdots, e^{j(M-1)\mu}]^T$, where $\mu = \frac{2\pi}{\lambda}\Delta_x \sin\theta_i$ with λ is the wavelength, Δ_x is the interelement spacing, and θ_i is the angle of arrival relative to the normal to the array axis. $\otimes$ denotes the Kronecker product. $\mathbf{f}(\tau_i) = \mathbf{v}(\tau_i) \odot \mathbf{s}$ where $\odot$ is the Schur product and

$$\mathbf{s} = [S(-K\Delta f), ..., S(-\Delta f), S(0), S(\Delta f), ..., S(K\Delta f)]^T, \tag{5}$$

where L=2K+1 and $S(f)$ is $sinc^2(fT_c)$ in the case of a rectangular chip waveform, for example. $\frac{1}{T_c}$ is the chip rate, $\mathbf{v}(\tau_i) = e^{-jK\nu}[1, e^{j\nu}, \cdots, e^{j2K\nu}]^T$, where $\nu = 2\pi\Delta f \tau_i$. Typically, $\Delta f = \frac{1}{\tau_{max}}$.

The "largest" generalized eigenvector of the asymptotic $ML \times ML$ matrix pencil $\{\mathbf{K}_{S+I}, \mathbf{K}_I\}$ is

$$\mathbf{w}_{opt} = \mathbf{K}_I^{-1}\mathbf{e}_s, \tag{6}$$

where $\mathbf{e}_s = \sqrt{\sigma_s}\sum_{i=1}^{K_d} g_i \mathbf{f}(\tau_i) \otimes \mathbf{a}(\theta_i)$. Thus, $\mathbf{e}_s = \mathbf{K}_I \mathbf{w}_{opt}$ and the $ML \times 1$ estimated signal vector

$$\hat{\mathbf{e}}_s = \hat{\mathbf{K}}_I \hat{\mathbf{w}}_{opt} \approx \sqrt{\sigma_s}\sum_{i=1}^{K_d} g_i \mathbf{f}(\tau_i) \otimes \mathbf{a}(\theta_i) \tag{7}$$

De-stacking the $M \times 1$ sub-vectors of $\hat{\mathbf{e}}_s$ through the $mat(\cdot)$ operator yields the $M \times L$ matrix:

$$\hat{\mathbf{E}}_s = mat(\hat{\mathbf{e}}_s) = mat(\hat{\mathbf{K}}_I \hat{\mathbf{w}}_{opt}) \approx \sqrt{\sigma_s}\sum_{i=1}^{K_d} g_i \mathbf{a}(\theta_i)\mathbf{f}^T(\tau_i) \tag{8}$$

We consider applying 2D Unitary ESPRIT to $\hat{\mathbf{E}}_s$ so that the final step yields eigenvalues of the form $\tan\left\{\frac{\mu_i}{2}\right\} + j\tan\left\{\frac{\nu_i}{2}\right\}$, where $\mu_i = \frac{2\pi}{\lambda}\Delta_x \sin\theta_i$ and $\nu_i = 2\pi\frac{\tau_i}{\tau_{max}}, i = 1. \cdots, K_d$. Before we can apply the 2D Unitary ESPRIT algorithm, we need to adjust the structure of $\hat{\mathbf{E}}_s$ such that the matrix exhibits the shift-invariance property along both the space and frequency dimensions. Since we know the spectrum of the chip waveform, we may divide out the "amplitude taper" represented by $\mathbf{s}$ in $\mathbf{f}(\tau_i) = \mathbf{v}(\tau_i) \odot \mathbf{s}$. To this end, define $\mathbf{\Gamma} = diag(\mathbf{s})$. Post-multiplying $\hat{\mathbf{E}}_s$ by $\mathbf{\Gamma}^{-1}$ yields

$$\hat{\mathbf{E}}_s' \approx \sqrt{\sigma_s}\sum_{i=1}^{K_d} g_i \mathbf{a}(\theta_i)\mathbf{v}^T(\tau_i) \tag{9}$$

However, we effectively have a single snapshot of 2D data and thus require 2D smoothing for extracting multiple snapshots. Note that the factor $e^{-jK\nu}$ in $\mathbf{v}(\tau_i)$ can be absorbed in g_i such that $\mathbf{a}(\theta_i)$ and $\mathbf{v}(\tau_i)$ both have Vandermonde structure which allows us to perform 2D smoothing. We propose two different orders of processing, pre-eigenanalysis 2D smoothing and post-eigenanalysis 2D smoothing, prior to applying 2D Unitary ESPRIT. These schemes are discussed below.

3.1. Post-eigenanalysis 2D smoothing

We need at least $K_d/2$ snapshots to handle K_d multipaths. Since there is effectively a single snapshot available after computing $\hat{\mathbf{e}}_s$, we can apply a 2D smoothing technique to $\hat{\mathbf{E}}_s'$ to extract $K_d/2$ or more identical rectangular subarrays out of the overall pseudo-array to get the effect of multiple snapshots. Note that the maximum number of sources 2D Unitary ESPRIT can handle is minimum $\{(m_1-1)m_2, m_1(m_2-1)\}$, given that the size of the subarray is $m_1 \times m_2$ and the number of extracted snapshots is $(M-m_1+1)\times(L-m_2+1)$. Therefore, these relationships must be satisfied: $min\{(m_1-1)m_2, m_1(m_2-1)\} \leq K_d$ and $(M-m_1+1)\times(L-m_2+1) \geq \frac{K_d}{2}$. Let $\mathbf{E}^{(m,l)}, 0 \leq m \leq (M-m_1), 0 \leq l \leq (L-m_2)$ denote the (m,l)-th extracted snapshot with dimension $m_1 \times m_2$. Applying the $vec(\cdot)$ operator, we stack the columns of $\mathbf{E}^{(m,l)}$ to form the $m_1 m_2 \times 1$ vector $\mathbf{e}^{(m,l)}$. We then form an $m_1 m_2 \times (M-m_1+1)(L-m_2+1)$ matrix $\mathbf{X} = [\mathbf{e}^{(0,0)}, \mathbf{e}^{(1,0)}, \cdots, \mathbf{e}^{(M-m_1, L-m_2)}]$ which plays the role of the data matrix needed for 2D Unitary ESPRIT. The subsequent steps of the 2D Unitary ESPRIT algorithm are easily applied to calculate $\{(\theta_i, \tau_i)\}, i = 1, \cdots, K_d$.

3.2. Pre-eigenanalysis 2D smoothing

As an alternative, we may effect 2D smoothing on each original space-frequency snapshot vector to generate multiple snapshots with lower dimension $m_1 \times m_2$ and form the smoothed version of the correlation matrix pencil denoted $\{\overline{\mathbf{K}}_{S+I}, \overline{\mathbf{K}}_I\}$. Note that we need to post-multiply each space-frequency snapshot by $\boldsymbol{\Gamma}^{-1}$ to achieve the required Vandermonde structure before performing 2D smoothing (This also facilitates use of forward-backward averaging). The effect of 2D smoothing is to "decorrelate" the multipaths such that we can choose the K_d $m_1 m_2 \times 1$ generalized "largest" eigenvectors of the smoothed version of $\{\mathbf{K}_{S+I}, \mathbf{K}_I\}$ as the K_d "snapshots". Denote $\mathbf{E} = [\mathbf{e}_1, \mathbf{e}_2, \cdots, \mathbf{e}_{K_d}]$, where $\mathbf{e}_i$ is the i-th "largest" generalized eigenvector of $\{\overline{\mathbf{K}}_{S+I}, \overline{\mathbf{K}}_I\}$. The subspace spanned by $\mathbf{X} = \overline{\mathbf{K}}_I \mathbf{E}$ will be the same as the subspace spanned by $\overline{\mathbf{A}} = [\overline{\mathbf{a}}(\theta_1, \tau_1), \cdots, \overline{\mathbf{a}}(\theta_{K_d}, \tau_{K_d})]$, where $\overline{\mathbf{a}}(\theta_i, \tau_i) = \mathbf{v}^{'}(\tau_i) \otimes \mathbf{a}^{'}(\theta_i), 1 \leq i \leq K_d$; the dimensions of $\mathbf{v}^{'}(\tau_i)$ and $\mathbf{a}^{'}(\theta_i)$ are $m_2 \times 1$ and $m_1 \times 1$, respectively. It follows that we can apply the 2D Unitary ESPRIT algorithm to the $m_1 m_2 \times K_d$ matrix $\mathbf{X}$ for joint AOA-delay estimation.

4. REDUCED DIMENSION PROCESSING VIA JOINT ANGLE-DELAY ESTIMATION

In this section, we develop the reduced dimension space-time 2D RAKE receiver related to [4] with knowledge of $\{(\theta_i, \tau_i)\}$. As substantiated in [4], reduced dimension processing offers faster convergence if the compression matrix is designed judiciously. For the given i-th AOA-delay pair (θ_i, τ_i), the optimal beamformer for the corresponding multipath arrival is given by the well-known Weiner solution $\mu_i \mathbf{R}_I^{-1} \mathbf{a}(\theta_i)$, where $\mu_i = \frac{1}{\mathbf{a}^H(\theta_i)\mathbf{R}_I^{-1}\mathbf{a}(\theta_i)}$ and $\mathbf{R}_I$ is the interference plus noise spatial correlation matrix. The approach is to optimally combine each multipath component after applying the optimal beamforming weight vector to the corresponding time sample of the multipath arrival at each antenna. The proposed reduced-dimension space-time RAKE receiver exploiting the estimates $\{(\hat{\theta}_i, \hat{\tau}_i)\}, i = 1, \cdots, K_d$, is as follows. We may rewrite the maximizing SINR criterion with the compression matrix $\mathbf{U}_r$ as:

$$\underset{\mathbf{w}_r}{\text{Maximize}} \quad \frac{\mathbf{w}_r^H \mathbf{K}_{S+I}^r \mathbf{w}_r}{\mathbf{w}_r^H \mathbf{K}_I^r \mathbf{w}_r},$$

where

$$\mathbf{K}_{S+I}^r = \mathbf{U}_r^H \hat{\mathbf{K}}_{S+I}^{st} \mathbf{U}_r \qquad \mathbf{K}_I^r = \mathbf{U}_r^H \hat{\mathbf{K}}_I^{st} \mathbf{U}_r, \tag{10}$$

and $\{\hat{\mathbf{K}}_{S+I}^{st}, \hat{\mathbf{K}}_I^{st}\}$ is the full dimension space-time matrix pencil, which is estimated in a similar way as in [3] by using time samples instead of the selected frequency samples. Note that the dimension of $\{\hat{\mathbf{K}}_{S+I}^{st}, \hat{\mathbf{K}}_I^{st}\}$ is $MN_s \times MN_s$. Making use of the estimated AOA-delay parameter pairs, we form the compression matrix $\mathbf{U}_r$ as:

$$\mathbf{U}_r = [\mu_1 \boldsymbol{\delta}_1 \otimes \hat{\mathbf{R}}_I^{-1} \mathbf{a}(\hat{\theta}_1) \vdots \cdots \vdots \mu_{K_d} \boldsymbol{\delta}_{K_d} \otimes \hat{\mathbf{R}}_I^{-1} \mathbf{a}(\hat{\theta}_{K_d})] \tag{11}$$

where $\mu_i = 1/\mathbf{a}^H(\theta_i)\mathbf{R}_I^{-1}\mathbf{a}(\theta_i)$ and

$$\hat{\mathbf{R}}_I = \frac{1}{N_s} \sum_{l=0}^{N_s-1} \boldsymbol{\Gamma}_l^T \hat{\mathbf{K}}_I^{st} \boldsymbol{\Gamma}_l \; ; \; \boldsymbol{\Gamma}_l = \begin{array}{cl} \begin{bmatrix} \mathbf{0} \\ \mathbf{I} \\ \mathbf{0} \end{bmatrix} & \begin{array}{l} (l-1)M \\ M \\ (N_s - l)M \end{array} \end{array} \tag{12}$$

and $\boldsymbol{\delta}_i = [0, \cdots, 0, 1, 0, \cdots .0]^T$ with the 1 in the i-th position corresponding to the time sample closest to the estimate of the relative delay of the i-th multipath arrival.

With the paired angle and delay estimated parameters, we can calculate the decision variable for each possible Walsh symbol at a given symbol period as:

$$\|\hat{\mathbf{w}}_r^H (\mathbf{U}_r^H \mathbf{x}_F^{(j)}(n))\|^2, j = 1, \cdots, 64, \tag{13}$$

where $\mathbf{x}_F^{(j)}(n)$ is a space-time snapshot from the j-th matched filter encompassing the "fingers" location (only one matched filter output actually has "fingers"), and $\hat{\mathbf{w}}_r$ is the "largest" generalized eigenvector of the "compressed" $K_d \times K_d$ matrix pencil $\{\hat{\mathbf{K}}_{S+I}^r, \hat{\mathbf{K}}_I^r\}$.

5. SIMULATION RESULTS

The simulations presented here employ IS-95 uplink signal model parameters, although our algorithms can be applied to classical DS-CDMA communication systems with either periodic or aperiodic spreading codes. The chip period is 0.8138 μs; the sampling rate was twice the chip rate; rectangular chip waveform was used. The number of half-chip spaced taps at each antenna used to encompass the delay spread was 16. The number of selected DFT samples was 9. $M = 8$ antennas were used. A three-ray multipath model was used for the desired user wherein the direct path arrived at an angle of 0^0 relative to broadside. The SNR's of the two specular multipaths were 1 and 3 dB below that the direct path and phase shifted by 90^0 and 45^0 at the array center, respectively.

Joint Angle-Delay Estimation:

Example 1. *near-far problem*: The MUAI parameters are listed in Table. 1 for the "near far" problem scenario. Figure 1 displays the estimated AOA and delay "scatter plots" obtained from 1000 independent runs with the matrix pencil $\{\hat{\mathbf{K}}_{S+I}, \hat{\mathbf{K}}_I\}$ averaged over 10 Walsh symbol periods, and the input SNR x of the direct path signal equal to -20 db. The subarray size (m_1, m_2) was chosen to be $(6, 5)$. It is observed that the scatter plots obtained with pre-eigenanalysis 2D smoothing are more localized than that obtained using post-eigenanalysis 2D smoothing. Also, some outliers were incurred in this simulation example using post-eigenanalysis 2D smoothing.

Example 2. *equal input power*: Here we create a simulation scenario with equal input power for all the co-channel users. The signal of the desired user is the same as the example 1. The input SNR x of the direct path was equal to -20db. The other 40 users with different PN codes and single path were created with input SNR equal to -20db, and the AOAs were uniformly distributed within 120°. Figure 2 displays the estimated AOA and delay "scatter plots" obtained from 500 independent runs. The other parameters are the same as those in Example 1.

Reduced Dimension Processing: Figure 3 displays a typical result of the 64 normalized decision variables with the "correct" Walsh symbol index marked with 'x' for a single trial run for both the reduced dimension and the full dimension 2D RAKE receiver conducted at x = -21db in Table 1. The pre-eigenanalysis 2D smoothing algorithm was used in estimating $\{(\theta_i, \tau_i)\}, i = 1, 2, 3$. Once the first three Walsh symbols have been estimated (using either a training sequence or some blind initialization algorithm which was discussed in [4]), $\hat{\mathbf{K}}_{S+I}$ and $\hat{\mathbf{K}}_I$ were averaged over the three past Walsh symbol periods using only the one matched filter output per symbol corresponding to the estimated symbol, and the "largest" generalized eigenvector was applied to each of the 64 Walsh correlator outputs generated for estimating the next Walsh symbol as in a decision directed mode of operation presented in [2]. It shows that a significant increase in separation between the value of the true Walsh symbol decision variable and the other 63 decision variables can be achieved by using the knowledge of the angle-delay estimates to effect reduced dimension processing. Note that the size of the full dimension space-time correlation matrix is 128 × 128. In contrast, the size of the reduced dimension correlation matrix is only 3 × 3. To demonstrate faster convergence with reduced dimension processing, Figure 4 displays the output SINRs of the

Table 1: Signal and MUAI parameters

	Signal	MUAI1	MUAI2	MUAI3
SNR 1,2,3	x,x-1,x-3db	x+20,x+10, - db	x+4,x+6, - db	x,x-3, - db
Phase 1,2,3	$0^o, 45^o, 90^o$	$45^o, 50^o, -$	$-30^o, -35^o, -$	$180^o, 170^o, -$
AOA 1,2,3	$0^o, 7^o, 14^o$	$50^o, 55^o, -$	$-20^o, -23^o, -$	$-10^o, -7^o, -$
Delay 1,2,3 ($\times \frac{1}{2} T_c$)	0,3,8	$0, 3, -$	$0, 6, -$	$0, 10, -$

full space-time processing and reduce dimension processing with AOA-delay estimates while the number of Walsh symbols for averaging $\hat{\mathbf{K}}_{S+I}$ and $\hat{\mathbf{K}}_I$ was varied from two to ten, and the input SNR x in Talble 1 of the direct path signal equal to -20 db.

6. CONCLUSION

Simulation results show that our algorithms can accurately estimate the AOA and delay for each multipath under "near-far" conditions. The AOA information is useful for FDD downlink beamforming and source localization for emergency service. The pre-eigenanalysis 2D smoothing algorithm offers better performance than the post-eigenanalysis 2D smoothing algorithm. The paired AOA and delay information may be used to reduce the dimensionality of the space-time 2D RAKE receiver. Our simulation results show that better separation between the value of the true Walsh symbol decision variable and the other 63 decision variables may be achieved by using the knowledge of the paired angle-delay estimates, as opposed to that obtained with full dimension space-time processing. This better performance results from the faster convergence toward the optimal weight vector due to the reduced dimensionality under conditions of limited available symbols where channel characteristics remain approximately stationary. The preliminary simulation results presented reveal the performance of the joint AOA-delay estimator and the resulting reduced space-time RAKE receiver to be quite promising. Future work includes the choice of subarray size employed in 2D smoothing and comparing the performance of the joint AOA-delay estimator to the CRB(Cramer-Rao Bound).

REFERENCES

[1] M. D. Zoltowski, M. Haardt, and C.P. Mathews, "Closed-form 2D angle estimation with rectangular arrays in element space or beam space via Unitary ESPRIT," *IEEE Trans. Signal Processing, vol. 44, pp.316-328,* Feb. 1996.

[2] M. D. Zoltowski, Y.F. Chen and J. Ramos, "Blind 2D RAKE Receiver Based on Space-Time Adaptive MVDR Processing for The IS-95 CDMA System," *Milcom '96*, McLean, VA, pp.618-622, Oct. 1996.

[3] M. D. Zoltowski and J. Ramos, "Blind Adaptive Beamforming for CDMA Based PCS/Cellular," *29th Asilomar IEEE Conf. on Signals, Systems, & Computers, pp.378-382,* Nov. 1995.

[4] Y.F. Chen and M. D. Zoltowski, " Convergence Analysis and Tracking Ability of Reduced Dimension Blind Space-Time Rake Receivers for DS-CDMA," *VTC '98*, pp.2333-2337, May 1998.

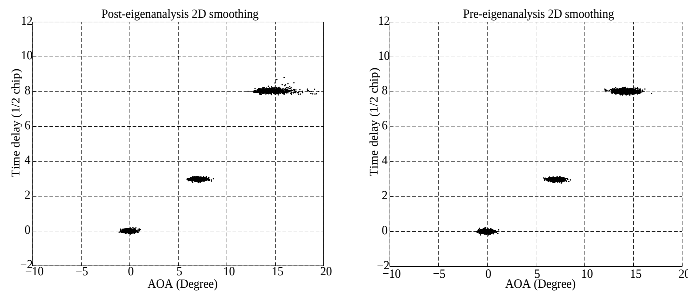

Figure 1: The estimates under "near-far" problem scenario

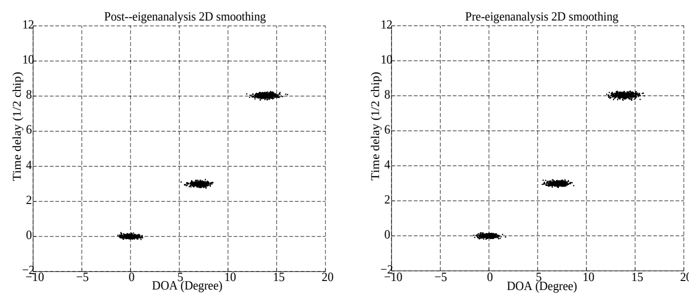

Figure 2: The estimates under equal input power scenario

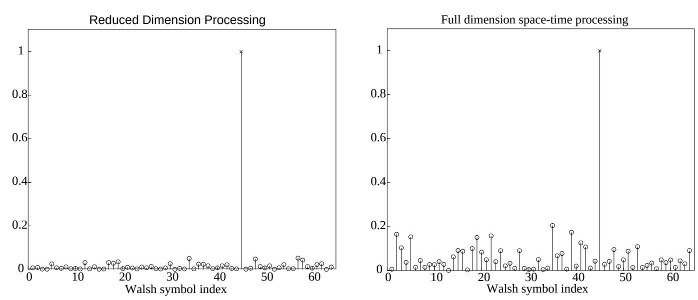

Figure 3: Typical result of the 64 decision variables

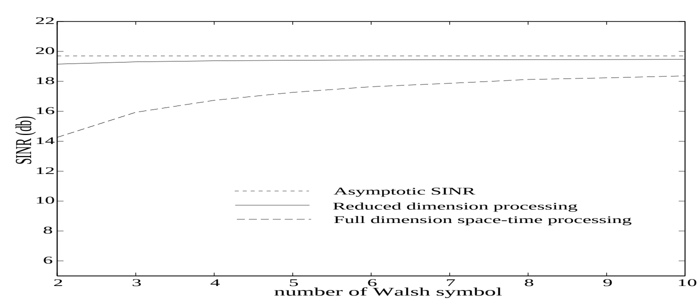

Figure 4: Convergence Comparison